On Combining Gait Features

Yasushi Makihara, Daigo Muramatsu, Haruyuki Iwama, and Yasushi Yagi
Osaka University
{makihara, muramatsu, iwama, yagi}@am.sanken.osaka-u.ac.jp

Abstract— **This paper describes a method of gait recognition using multiple gait features in conjunction with score-level fusion techniques. More specifically, we focus on the state-of-the-art period-based gait features such as a gait energy image, a frequency-domain feature, a gait entropy image, a chrono-gait image, and a gait flow image. In addition, we employ various types of the score-level fusion approaches including not only conventional transformation-based approaches (e.g., sum-rule and min-rule) but also classification-based approaches (e.g., support vector machine) and density-based approaches (e.g., Gaussian mixture model, kernel density estimation, linear logistic regression). In experiments, the large-population gait database with 3,249 subjects was used to measure the performance improvement in a statistically reliable way. The experimental results show 7% relative improvement on average with regard to equal error rate of the false acceptance rate and false rejection rate in verification scenarios, and also show 20% reduction of the number of candidates to be checked under 1% misdetection rate on average in screening tasks.**

I. Introduction

Gait recognition [51] has recently gained considerable attention as a promising biometric verification/identification method for surveillance systems, owing to its ability of ascertaining identity from a distance. In fact, the gait recognition has been applied to CCTVs in the street and served as a biometric evidence in the forensic science field [67], [8]. The performance of the gait recognition is, however, often degraded by various intra-subject variations caused by views [26], [41], [31], walking speeds [43], [30], clothing [23], carrying status [66], surfaces [58], and elapsed time [45].

In order to overcome such difficulties, information fusion techniques have been brought into gait recognition. One of typical approaches is combining multiple modalities. In particular, fusion of gait and face biometrics has been actively studied [60], [27], [34], [80], [81], [22] because the both modalities are acquired from the same device, namely, a camera. These types of fusion approaches do, however, not work efficiently when the image resolution of a face is too small to be recognized.

Another way is combining evidences from multiple views, which are acquired from multiple cameras [14], [75], [79] or view variations in a single wide view-range camera [65]. The multi-view observations are also used for improving the performance of view-invariant gait recognition [61], [42], [29], [19]. It is, however, not always available the multi-camera settings with sufficient view overlaps and/or long-term image sequences with sufficient view variations.

On the other hands, in the context of a single-observation matching, part-based gait recognition approaches could be regarded as one of fusion approaches. In these approaches, the whole body is divided into multiple parts based on human model fitting or anatomical knowledge and scores from the individual body parts are fused [14], [9], [35], [23].

Moreover, multi-algorithm fusion could be a potential approach, which has been widely studied in the other biometric modalities (e.g., fingerprint [62], [10], iris [59], [73], and face [15], [11], [55]). Although a variety of individual gait recognition algorithms have been proposed [52], [48], [47], [14], [74], [37], [18], [41], [4], [5], [33], [71], [21], to the best of our knowledge, there are few studies on combining these multiple gait recognition algorithms for improving performance.

Therefore, we tackle with the multi-algorithm fusion on the gait recognition in this paper. In particular, we focus on multiple state-of-the-art period-based gait features [18], [41], [4], [33], [71]. Moreover, whereas the existing fusion approaches to the gait recognition employ relatively simple techniques such as sum-rule and min-rule, we explore various types of state-of-the-art score-level fusion techniques ranging from transformation-based approaches [28] to classification-based and density-based approaches [72], [49], [68], [1], [39]. In experiments, all the combinations of the gait features and the score-level fusion techniques are evaluated with a large-population gait database with 3,249 subjects in a statistically reliable way, and then the upper bound of the gait recognition performance is pursued.

The reminder of this paper is organized as follows. Section II gives a summary on related techniques on the gait recognition and the score-level fusion, respectively. Brief descriptions on the state-of-the-art gait features and score-level fusion approaches used in this paper are given in section III and IV, respectively. The experiments for all the combinations of the gait features and the score-level fusion approaches are conducted in section V and concluding remarks and future work are given in section VI.

II. Related Work

A. Gait recognition

Approaches to the gait recognition mainly fall into two families: model-based and appearance-based (or model-free) approaches. The model-based approaches usually fit articulated human-body models to observed images and kinematic parameters (e.g., joint angle sequences) as well as static parameters (e.g., torso and leg lengths) are extracted as gait features. For examples, while Bobick and Johnson [7] extract torso and leg lengths as well as strides with the three-linked model, Cunado et al. [13] and Yam et al. [76] extract joint angle sequences of legs with the pendulum model in conjunction with Fourier analysis. Urtasun and Fua [69] exploit a 3D human model with volumetric primitives of links, and Yang et al. [77] exploit a 3D human model with cylindrical links. As a more mechanical model, Ariyanto and Nixon [2] propose a marionette mass-spring model for 3D gait recognition. While the model-based approaches have several advantages over the appearance-based ones in terms of view invariance and clothing invariance, they often suffer from model fitting errors and relatively high computational cost. Therefore, the appearance-based approaches often outperform the model-based ones in general, which is the main reason why the most of the gait recognition approaches adopt the appearance-based ones.

The appearance-based approaches extract gait features directly from images, typically from size-normalized silhouette images, without the model. Gait features used in this family further fall into two classes: frame-based and period-based gait features. The frame-based gait features are naturally extracted frame-by-frame and frame synchronization or phase (gait stance) estimation follows in matching stage. Sarkar et al. [58] propose a direct silhouette sequence matching as a baseline method, while the Murase and Sakai [48] and Mori et al. [46] employ a parametric eigen space to represent a periodic gait silhouette sequence. Liu et al. [38] propose a gait dynamics normalization by using a population hidden Markov model to match two silhouettes at the same phase. Beyond the raw silhouette sequences, Contour et al. [14] project the silhouette into a width vector and Liu et al. [36] project it into a frieze pattern, namely, combination of width and height vectors. The frame-based features are, however, relatively susceptible to silhouette noise and also frame synchronization process is considerably time consuming.

On the other hands, the period-based gait features are computed by integrating over all the frames within a detected period, which makes the extracted gait feature robust to pixel-by-pixel independent noise [18]. The simplest yet the most prevailing one is a gait energy image (GEI) [18] otherwise known as an averaged silhouette [37] which is computed by just averaging the silhouette value pixel-by-pixel over the gait period. Considering the periodic property of gait, a frequency-domain feature (FDF) [41] is computed as pixel-by-pixel amplitude spectra of zero-, one-, and two-times frequency elements. As a variant of the GEI, a gait entropy image (GEnI) [4] is computed as pixel-by-pixel entropy of the GEI so as to focus on dynamic regions. A gait flow image (GFI) [33] more directly focus on the dynamic components, where the optical flow lengths observed on the silhouette contour are averaged over the gait period. As another way of motion representation, a chrono-gait image (CGI) [71] assigns the color to the silhouette contour based on *phase* (e.g., blue to single support phase and red to double support phase), and average them over the quarter gait period. Beside the above gait features, many of the gait features such as a masked GEI [5], a Gabor filter-based feature [66], a motion silhouette image [32], a self-similarity plot [6], and a Fourier descriptor [47], have been also proposed to date. There are, however, no attempts to combine the excellent period-based gait features for improving the performance.

B. *Score-level fusion*

Approaches to the score-level fusion fall into three families: (1) transformation-based approaches [28], [25], [64], (2) classification-based approaches [20], and (3) density-based approaches [49], [1], [16], [39].

In the transformation-based approaches, scores are first mapped onto a common domain by normalization techniques (e.g., z-normalization [3], F-normalization [54], EER-normalization [17], log likelihood-based normalization [56], or quality-based normalization [57]) and are then combined using various rules (e.g., sum-rule and min-rule [28]) to provide a fused score.

In the classification-based approaches, multiple scores are treated as feature vectors and a classifier (e.g., neural network [12] or support vector machine (SVM) [72]) is constructed to discriminate each class. The signed distance from the decision boundary is usually regarded as the fused score.

While these two families of approaches do not guarantee the optimality in terms of receiver operating characteristics (ROC) in verification scenarios, the density-based approaches guarantee the optimal fusion as long as the probability density function (PDF) of the score given for each class is correctly computed [50].

The density-based approaches are further categorized in terms of two aspects of the distribution representation: (A) parametric or non-parametric approaches, and (B) generative or discriminative approaches. The parametric and generative approaches assume certain PDF models (e.g., Gaussian mixture model (GMM)) for each class separately and estimate the parameters of the model from the training samples [49]. The parametric and discriminative approaches bypass estimation of the individual PDFs and directly model a function of the likelihood ratio or posterior (e.g., linear logistic regression (LLR) of the likelihood ratio) [1]. These parametric approaches work well if the assumed models closely fit the actual distributions; otherwise they fail.

On the other hands, the non-parametric approaches represent the distributions using histogram bins or control points. Some of the non-parametric and generative approaches assume the independence of each dimensional score and represent a joint PDF as the product of each dimension of the PDFs computed by kernel density estimation (KDE) [16]. The non-parametric and discriminative approaches usually allocate lattice-type control points on the multi-dimensional score space, allowing a function of the posteriors on the control points to be estimated [39].

As seen above, although a wide variety of approaches to the score-level fusion have been proposed to date, only relatively simple approaches (e.g., sum-rule and min-rule from the transformation-based approaches) have been applied to the gait recognition. Therefore, it is worth investigating the performance of the multi-algorithm gait recognition not only by such simple transformation-based approaches but also

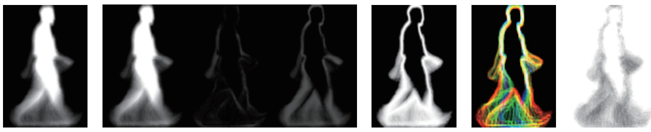

(a) GEI (b) FDF (c) GEnI (d) CGI (e) GFI

Fig. 1. Gait features

by the other state-of-the-art classification-based and density-based approaches.

III. Gait Features

A. Preprocessing

Given a input image sequence, a gait silhouette sequence is extracted by background subtraction-based graph-cut segmentation [44]. The gait silhouette sequence is then scaled and registered so as to generate a size-normalized gait silhouette sequence, whose width and height are $W = 88$ pixels and $H = 128$ pixels, respectively. The pixel value at the position (x,y) at the t-th frame in the size-normalized silhouette sequence is denoted as $I(x,y,t)$, where 0 and 1 correspond to background and foreground, respectively. Finally, the gait period P is detected by maximizing a normalized autocorrelation of the silhouette sequence [41].

B. Gait energy image (GEI)

The GEI [18] (Fig. 1(a)) is simply computed by averaging the pixel values over the gait period as

$$GEI(x,y) = \frac{1}{P}\sum_{t=1}^{P} I(x,y,t). \tag{1}$$

C. Frequency-domain feature (FDF)

Regarding the gait period P as a base period for Fourier analysis, the FDF [41] (Fig. 1(b)) is computed as amplitude spectra

$$FDF(x,y,k) = \frac{1}{P}\left|\sum_{t=1}^{P} I(x,y,t)e^{-j\omega_0 kt}\right|, \tag{2}$$

where ω_0 is a base angular frequency for the gait period P, and $FDF(x,y,k)$ is the amplitude spectrum for the k-time frequency $(k = 0,1,2)$ at the position (x,y). Note that the amplitude spectra for the 0-time frequency (direct currency elements) are identical to the GEI.

D. Gait entropy image (GEnI)

The GEnI [4] (Fig. 1(c)) is computed to emphasize the dynamic areas as

$$GEnI(x,y) = -z\log_2 z - (1-z)\log_2(1-z), \tag{3}$$

where $GEnI(x,y)$ is Shannon entropy for $z = GEI(x,y)$, that is, the GEI value at the position (x,y).

E. Chrono-gait image (CGI)

The CGI [71] (Fig. 1(d)) is computed by averaging the colored contour image, whose color is assigned based on the phase, as

$$CGI(x,y) = \frac{1}{p}\sum_{i=1}^{p} PG_i(x,y), \tag{4}$$

where p is the quarter gait periods, $PG_i(x,y) = \sum_{t=1}^{n_i} C(x,y,t)$, is the sum of the total n_i colored contour images in the i-th quarter gait period, and $C(x,y,t)$ is the colored gait contour value at the position (x,y) at the t-th frame.

F. Gait flow image (GFI)

The GFI [33] (Fig. 1(e)) is computed by averaging the optical flow lengths over the gait period as

$$GFI(x,y) = \frac{1}{P-1}\sum_{t=1}^{P-1} \|v(x,y,t)\|, \tag{5}$$

where $v(x,y,t)$ is the optical flow from t-th frame to $(t+1)$-th frame at the position (x,y).

IV. Score-level Fusion

A. Score normalization as preprocess

Normalizing the scale of each dimensional score is essential part for the success of the score-level fusion. In this paper, the z-normalization is applied to each probe so as that the average and the standard deviation of scores over all the galleries be 0 and 1, respectively. It is well known that this kind of probe-dependent z-normalization dramatically improves the ROC in a verification scenario (one-to-one matching) [53].

B. Sum-rule (Sum)

The sum-rule [28] is the representative of the non-training transformation-based approaches. Summation of the multiple scores is provided as a single fused score.

C. Min-rule (Min)

The min-rule [28] is also frequently used in the context of the transformation-based approaches. The minimum of the multiple scores is provided as a single fused distance.

D. Support vector machine (SVM)

The SVM [72] is one of typical classification-based approaches. Once the multiple scores are concatenated into a single feature vector, the SVM is learnt by using positive and negative training samples in the feature space. In the test phase, a signed distance to the decision boundary of the learnt SVM is provided as a single fused score. In this paper, linear and radial basis function (RBF) kernels are exploited and the hyper-parameters are trained via cross validation.

E. Gaussian mixture model (GMM)

The GMM [49] falls into the parametric and generative density-based approaches. The GMMs are trained for positive and negative samples separately by the EM algorithm so as to maximize the likelihood. The number of the components of the GMM is decided based on the minimum description length (MDL) criteria. The likelihood ratio or posterior is provided as a single fused score.

F. Linear logistic regression (LLR)

The LLR [1] falls into the parametric and discriminative density-based approaches. The linear logistic function of likelihood ratio is defined and its linear-term coefficients are computed so as that a loss function be minimized. The value of the linear logistic function is provided as a single fused score.

G. Kernel density estimation (KDE)

The KDE [16] falls into the non-parametric and generative density-based approaches. PDFs of the positive and negative samples are estimated for each dimensional score independently by kernel density estimator, and the joint distribution is computed as their product under an assumption of score independence. A bandwidth of the kernel function is automatically selected based on [70]. The likelihood ratio or posterior is provided as a single fused score.

H. Lattice-type control point (LCP)

The LCP [39] falls into the non-parametric and discriminative density-based approaches. The LCPs are allocated in the multiple score domain, and the posterior on the LCPs are directly estimated so as to minimize an objective function composed of data and smoothness terms. The smoothness coefficient λ is set to 1 in this paper. The posterior interpolated by the adjacent LCPs is provided as a single fused distance.

V. Experiments

A. Data sets

Because sufficient number of positive and negative samples are required for the success of the statistically reliable performance evaluation, we employed the OU-ISIR Biometric Score Database, Set 4 with Protocol 1 (BSS4-P1)[1]. derived from the large-population gait database [24] was employed. More specifically, 3,249 subjects joined the experiments and two walking image sequences were captured for each subject, which were assigned to a probe and a gallery, respectively. The state-of-the-art gait features, namely, GEI, FDF, GEnI, CGI, and GFI, were extracted from each of the sequences and then Euclidean distances for all the combinations of probes and galleries were computed as dissimilarity scores, which constructed a dissimilarity score matrix accompanied with probe and gallery IDs.

Thereafter, the whole set was randomly divided into two disjoint subsets: a training (development) set with 1,625 subjects and a test (evaluation) set with 1,624 subjects. Subsequently, dissimilarity score sub-matrices were extracted and the z-normalization [53] was applied to the training and test sets, respectively. Dissimilarity scores for pairs of the same and different subjects were extracted as positive and negative samples, respectively, from each of the training and test sets. As a result, while the training set contained 1,625 positive samples and 2,639,000 negative samples, the test set contained 1,624 positive samples and 2,635,752 negative samples. Thereafter, the training set was used for learning each of the training-based score-level fusion methods, and the test set was used for the performance evaluation.

Although we notice the existence of the other publicly available gait databases [58], [63], [78], [40] with a variety of covariates (e.g., view, walking speed, clothing, and shoe variations), the number of subjects in such databases is at most a hundred order and hence the statistical reliability of the performance evaluation on the score-level fusion could be significantly degraded. In this paper, we rather focus on the statistically reliable performance evaluation than the covariates, and then pursue the upper bound of the performance without such covariates. Performance analysis against the covariates is left as future work.

B. Score distributions

It is well known that the efficiency of the score-level fusion is dependent on the correlation between the score distribution. More specifically, the stronger the positive correlation is, the less the efficiency of the score-level fusion is. Conversely, the more independent the distribution is, the more the efficiency is. Therefore, in this section, the dissimilarity score distribution for all the combinations of two gait features are investigated as shown in Fig. 2.

As a result, because the GEI, FDF, and GEnI are silhouette region-based gait features, each combination of them have relatively strong correlation (Fig. 2(a)(b)(e)). In particular, the FDF completely contains the GEI as the direct currency component, the score distribution for GEI-FDF is quite strongly correlated (Fig. 2(a)).

On the other hands, the CGI and GFI are silhouette contour-based gait features and capture more dynamic components, and hence the correlation between the CGI/GFI and another gait feature is relatively weak (Fig. 2(c)(d)(f)(g)(h)(i)(j)). In particular, the score distribution correlation for CGI-GFI (Fig. 2(j)) is the weakest among all the combinations.

C. Performance evaluation in verification scenarios

In this section, performance in verification scenarios (one-to-one matching) is evaluated. For this purpose, we employed the ROC curve which indicate the tradeoff between the false rejection rate (FRR) of the genuine and the false acceptance rate (FAR) of the imposter when an acceptance threshold changes. The ROC curves for all the combinations are shown in Fig. 3. Moreover, an equal error rate of the FAR and FRR and its relative improvement rate to the best of the two gait features are summarized in Fig. 4.

[1]The OU-ISIR Biometric Score Database is publicly available at http://www.am.sanken.osaka-u.ac.jp/BiometricDB/BioScore.html

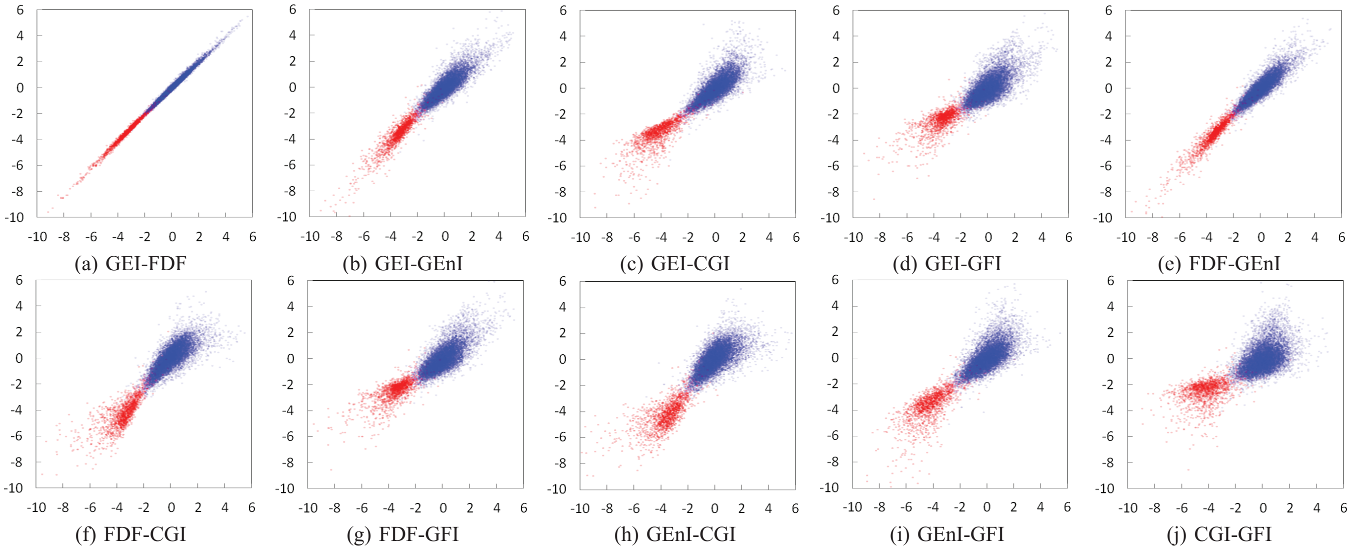

Fig. 2. Dissimilarity score distributions between two gait features. Horizontal and vertical axes indicate z-normalized distance for the first and the second gait features (e.g., GEI and FDF in (a)), respectively. Positive and negative samples are depicted by red and blue plots, respectively.

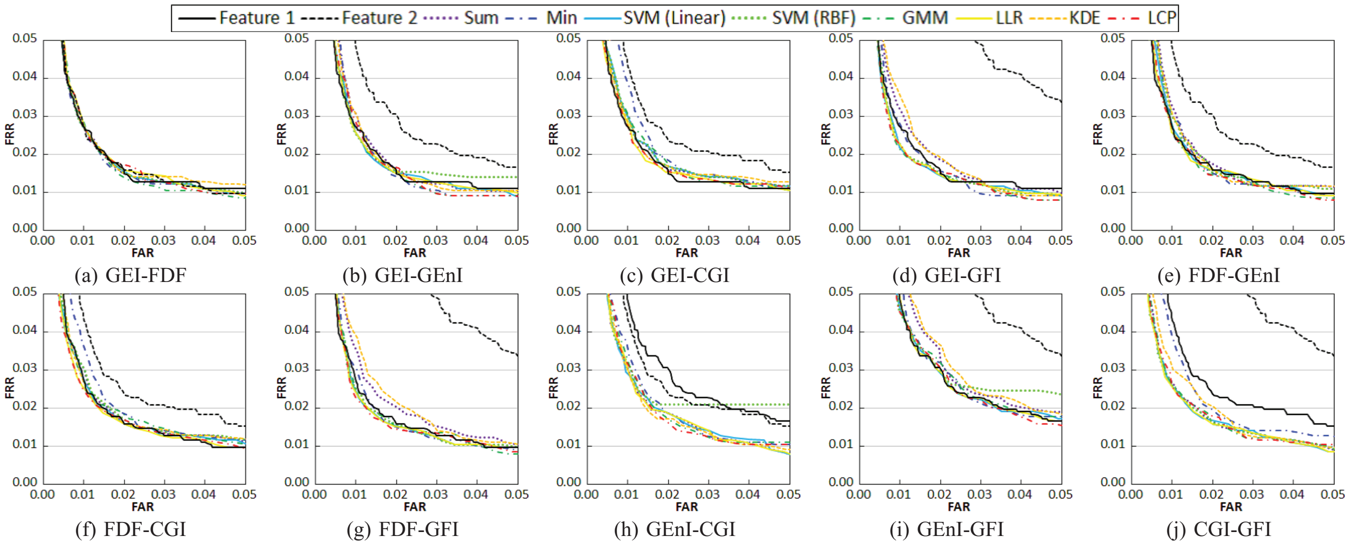

Fig. 3. ROC curves for score-level fusion of two gait features. Feature 1 and 2 corresponds to gait features denoted before and after hyphen (e.g., in (a), Feature1 is GEI, Feature 2 is FDF). It can be said that the score-level fusion works well when the colored lines (fusion) are lower than both of the black lines (single features).

As a result, it turns out that the score-level fusion improves the performance little for the strongly correlated combination, namely, GEI-FDF, GEI-GEnI, and FDF-GEnI. On the other hands, the score-level fusion clearly improves the performance for the combination with relatively weak correlation, namely, GEnI-CGI and CGI-GFI (relatively 20% w.r.t. EER). In addition, some of the score-level fusion approaches slightly improve the performance for the combination GEI-GFI and FDF-GFI (relatively 7% w.r.t. EER), while they little improve for the combination GEI-CGI, FDF-CGI, and GEnI-GFI.

Focused on the performance difference by the score-level fusion approaches, Sum and KDE sometimes fail (e.g., GEI-GFI and FDF-GFI) and hence their averaged performances are worse. On the other hands, SVM (Linear), LLR, and LCP constantly achieve the good performance, and hence their averaged performance are better, which demonstrates the effectiveness of the use of the state-of-the-art score-level fusion techniques.

Finally, while the best performance by the single gait feature is 1.79% EER (GEI or FDF), the best performance by the combination is 1.67% EER (GEI-GFI with SVM (Linear) or LCP, and FDF-GFI with SVM (Linear), LLR, or LCP). It is interesting that combination GEI-GFI or FDF-GFI achieves the best performance due to its relatively weak correlation, nevertheless the performance of the GFI is the worst (4.0% EER) among the single gait features.

D. Performance evaluation in identification scenarios

In this section, performance in identification scenarios (one-to-many matching) is evaluated. For this purpose, we employed the CMC curve which indicates the rates that the genuine subjects are included within each of ranks. The CMC curves for all the combinations are shown in Fig. 5. Moreover, the rank-1 identification rate and its relative

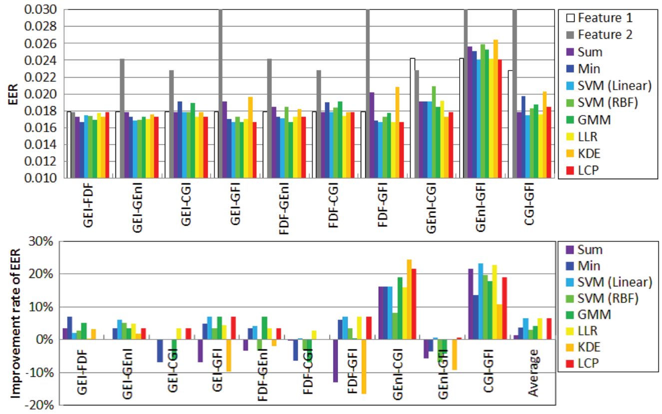

Fig. 4. EERs (top) and its relative improvement rate to the best of the two gait features (bottom). Feature 1 and 2 corresponds to gait features denoted before and after hyphen. In case of GEI-GEnI, the performance of the GEI is better than that of the GEnI, the relative improvement rate is measured to that of the GEI.

improvement rate to the best of the two gait features are summarized in Fig. 6. In addition, by considering a screening task, rank over 99% identification rate, in other words, below 1% misdetection rate, and its reduction rate to the best of the two gait features are summarized in Fig. 7. Note that the rank here means the number of candidates to be checked to keep 1% misdetection rate, and hence the rank reduction rate implies the reduction rate of the burden by surveillance agents.

As a result, in terms of rank-1 identification rate, the score-level fusion almost does not work except for the combination GEnI-CGI and CGI-GFI. In particular, the non-parametric density-based approaches (KDE and LCP) significantly degrade their performances.

On the other hands, in terms of the screening task, we can see the significant improvements by the score-level fusion. In fact, from 30% to 40% rank reduction rate are achieved for some of the combinations (e.g., GEI-GFI, FDF-GFI, GEnI-CGI). Moreover, it is quite interesting that the LCP achieves the best rank reduction rate on average (approximately 20%), while its rank-1 identification rate is considerably worse than the other approaches.

Therefore, the score-level fusion of multiple gait features is effective for the screening task, while it is not true to identification rates for lower ranks.

VI. Conclusion

This paper described a method of gait recognition using multiple gait features in conjunction with the score-level fusion techniques. All the pairs of the five state-of-the-art period-based gait features, namely, the GEI, FDF, GEnI, CGI, and GFI were evaluated with the eight score-level fusion approaches, that is, the sum-rule and min-rule as the transformation-based approaches, the SVM with linear and RBF kernel as the classification-based approaches, and the GMM, LLR, KDE, and LCP as the density-based approaches. The experiments with the large-population gait database of 3,249 subjects demonstrated that the score-level fusion of the two gait features with relatively weak correlation achieved the performance improvement with regard to EER in the verification scenarios and also reduced the candidates to be checked in a screening task.

While this paper pursued the upper bound of the performance by the score-level fusion of the multiple state-of-the-art gait features without covariates (e.g., view, walking speed, clothing, and shoes), the performance evaluation involving the covariates is one of important future work. In addition, because the identification rates for lower ranks in the identification scenarios were little improved by the score-level fusion, a study of the score-level fusion approach which focuses on lower-rank identification rates is another future work.

Acknowledgments

This work was partly supported by JSPS Grant-in-Aid for Scientific Research(S) Grant Number 21220003, "R&D Program for Implementation of Anti-Crime and Anti-Terrorism Technologies for a Safe and Secure Society", Strategic Funds for the Promotion of Science and Technology of the Ministry of Education, Culture, Sports, Science and Technology, the Japanese Government, and the JST CREST "Behavior Understanding based on Intention-Gait Model" project.

References

[1] F. Alonso-Fernandez, J. Fierrez, D. Ramos, and J. Ortega-Garcia. Dealing with sensor interoperability in multi-biometrics: the upm experience at the biosecure multimodal evaluation 2007. In *Proc. of SPIE 6994, Biometric Technologies for Human Identification IV*, Orlando, FL, USA, Mar. 2008.

[2] G. Ariyanto and M. Nixon. Marionette mass-spring model for 3d gait biometrics. In *Proc. of the 5th IAPR Int. Conf. on Biometrics*, pages 354–359, March 2012.

[3] R. Auckenthaler, M. Carey, and H. Lloyd-Thomas. Score normalization for text-independant speaker verification systems. *Digital Signal Processing*, 10(1-3):42–54, 2000.

[4] K. Bashir, T. Xiang, and S. Gong. Gait recognition using gait entropy image. In *Proc. of the 3rd Int. Conf. on Imaging for Crime Detection and Prevention*, pages 1–6, Dec. 2009.

[5] K. Bashir, T. Xiang, and S. Gong. Gait recognition without subject cooperation. *Pattern Recognition Letters*, 31(13):2052–2060, Oct. 2010.

[6] C. BenAbdelkader, R. Culter, H. Nanda, and L. Davis. Eigengait: Motion-based recognition people using image self-similarity. In *Proc. of Int. Conf. on Audio and Video-based Person Authentication*, pages 284–294, 2001.

[7] A. Bobick and A. Johnson. Gait recognition using static activity-specific parameters. In *Proc. of IEEE Conf. on Computer Vision and Pattern Recognition*, volume 1, pages 423–430, 2001.

[8] I. Bouchrika, M. Goffredo, J. Carter, and M. Nixon. On using gait in forensic biometrics. *J. of Forensic Sciences*, 56(4):882–889, 2011.

[9] N. Boulgouris and Z. Chi. Human gait recognition based on matching of body components. *Pattern Recognition*, 40(6):1763–1770, 2007.

[10] R. Cappelli, D. Maio, and D. Maltoni. A multi-classifier approach to fingerprint classification. *Pattern Analysis and Applications*, 5:136–144, 2002.

[11] N. V. Chawla and K. W. Bowyer. Designing multiple classifier systems for face recognition. In *Proceedings of the 6th Int. Conf. on Multiple Classifier Systems*, MCS'05, pages 407–416, Berlin, Heidelberg, 2005. Springer-Verlag.

[12] C. Chen and C. Chu. Fusion of face and iris features for multimodal biometrics. In *Proc. of Int. Conf. on Biometrics 2006*, pages 571–580, Hong Kong, China, Jan. 2006.

[13] D. Cunado, M. Nixon, and J. Carter. Automatic extraction and description of human gait models for recognition purposes. *Computer Vision and Image Understanding*, 90(1):1–41, 2003.

[14] N. Cuntoor, A. Kale, and R. Chellappa. Combining multiple evidences for gait recognition. In *Proc. of IEEE Int. Conf. on Acoustics, Speech, and Signal Processing*, volume 3, pages 33–36, 2003.

[15] J. Czyz, J. Kittler, and L. Vandendorpe. Multiple classifier combination for face-based identity verification. *PATTERN RECOGNITION*, 37(7):1459–1469, July 2004.

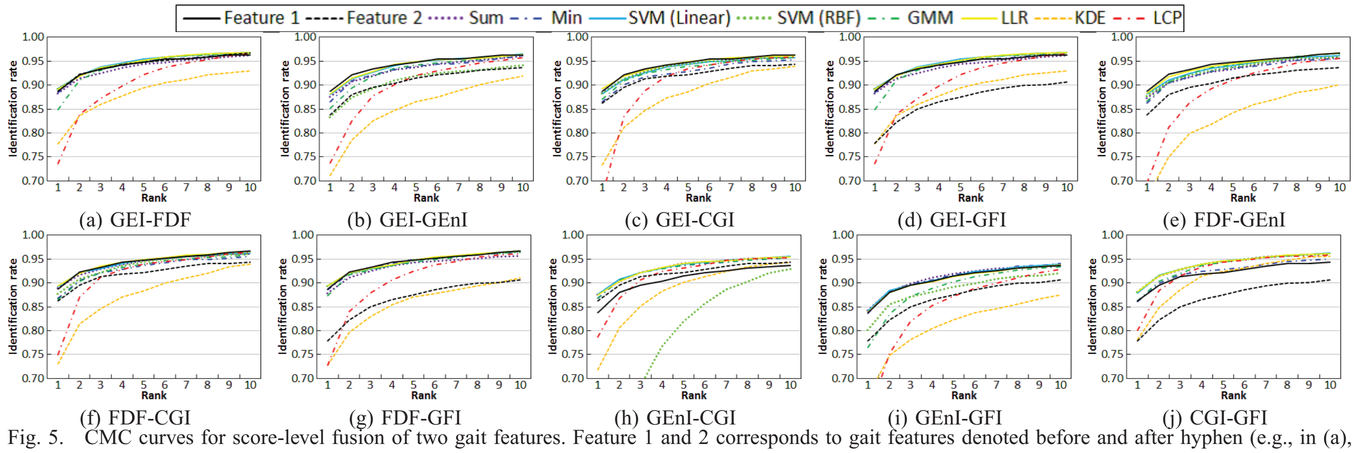

Fig. 5. CMC curves for score-level fusion of two gait features. Feature 1 and 2 corresponds to gait features denoted before and after hyphen (e.g., in (a), Feature1 is GEI, Feature 2 is FDF). It can be said that the score-level fusion works well when the colored lines (fusion) are higher than both of the black lines (single features).

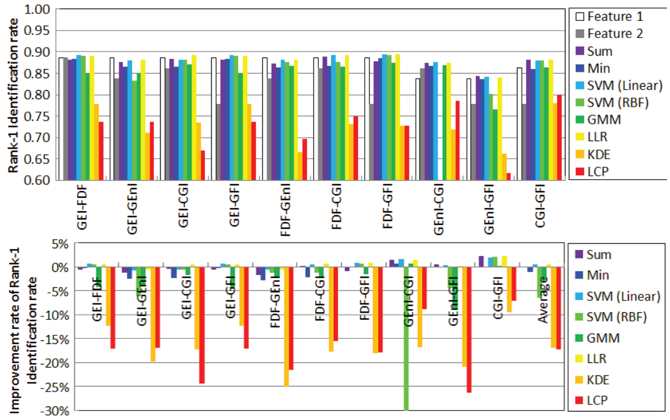

Fig. 6. Rank-1 identification rate (top) and its relative improvement rate to the best of the two gait features (bottom). Feature 1 and 2 corresponds to gait features denoted before and after hyphen.

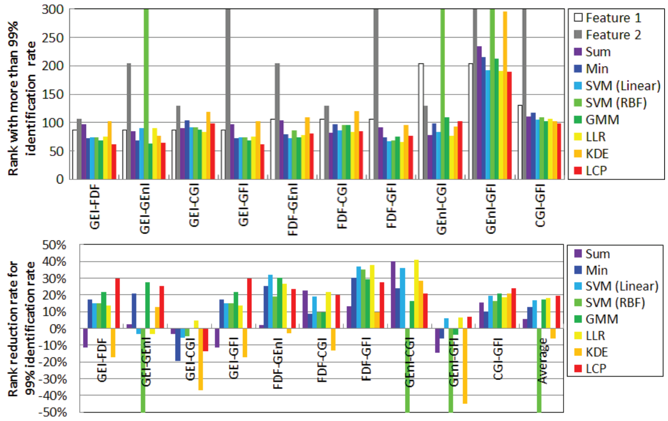

Fig. 7. Rank over 99% identification rate (top) and its reduction rate over the best of the two gait features (bottom). Feature 1 and 2 corresponds to gait features denoted before and after hyphen.

[16] S. C. Dass, K. Nandakumar, and A. K. Jain. A principled approach to score level fusion in multimodal biometric systems. In *Proc. of the 5th Int. Conf. on Audio- and Video-Based Biometric Person Authentication*, pages 1049–1058, Ny, USA, July 2005.

[17] J. Fierrez-Aguilar, J. Ortega-Garcia, and J. Gonzalez-Rodriguez. Target dependent score normalisation techniques and their application to signature verification. In *In LNCS 3072, Int'l Conf. on Biometric Authentication (ICBA)*, pages 498–504, Hong Kong, 2004.

[18] J. Han and B. Bhanu. Individual recognition using gait energy image. *IEEE Trans. on Pattern Analysis and Machine Intelligence*, 28(2):316–322, 2006.

[19] J. Han, B. Bhanu, and A. Roy-Chowdhury. A study on view-insensitive gait recognition. In *Proc. of IEEE Int. Conf. on Image Processing*, volume 3, pages 297–300, Sep. 2005.

[20] M. He, S. J. Horng, P. Fan, R. S. Run, R. J. Chen, J. L. Lai, M. Khan, and K. O. Sentosa. Performance evaluation of score level fusion in multimodal biometric systems. *Pattern Recognition*, 43(5):1789–1800, May 2010.

[21] M. Hofmann, S. Bachmann, and G. Rigoll. 2.5d gait biometrics using the depth gradient histogram energy image. In *Proc. of the 5th IEEE Int. Conf. on Biometrics Theory, Applications, and Systems*, pages Paper ID 172, 1–5, Washington D.C., USA, Sep. 2012.

[22] M. Hofmann, S. M. Schmidt, A. Rajagopalan, and G. Rigoll. Combined face and gait recognition using alpha matte preprocessing. In *Proc. of the 5th IAPR Int. Conf. on Biometrics*, pages 1–8, New Delhi, India, Mar. 2012.

[23] M. A. Hossain, Y. Makihara, J. Wang, and Y. Yagi. Clothing-invariant gait identification using part-based clothing categorization and adaptive weight control. *Pattern Recognition*, 43(6):2281–2291, Jun. 2010.

[24] H. Iwama, M. Okumura, Y. Makihara, and Y. Yagi. The ou-isir gait database comprising the large population dataset and performance evaluation of gait recognition. *IEEE Trans. on Information Forensics and Security*, 7(5):1511–1521, Oct. 2012.

[25] A. K. Jain, K. Nandakumar, and A. Ross. Score normalization in multimodal biometric systems. *Pattern Recognition*, 38(12):2117–2127, December 2005.

[26] A. Kale, A. Roy-Chowdhury, and R. Chellappa. Towards a view invariant gait recognition algorithm. In *Proc. of IEEE Conf. on Advanced Video and Signal Based Surveillance*, pages 143–150, 2003.

[27] A. Kale, A. Roy-Chowdhury, and R. Chellappa. Fusion of gait and face for human identification. In *Proc. of the IEEE Int. Conf. on Acoustics, Speech, and Signal Processing 2004 (ICASSP'04)*, volume 5, pages 901–904, 2004.

[28] J. Kittler, M. Hatef, R. P. W. Duin, and J. Matas. On combining classifiers. *IEEE Trans. on Pattern Analysis and Machine Intelligence*, 20(3):226–239, Mar. 1998.

[29] W. Kusakunniran, Q. Wu, J. Zhang, and H. Li. Support vector regression for multi-view gait recognition based on local motion feature selection. In *Proc. of IEEE computer society conference on Computer Vision and Pattern Recognition 2010*, pages 1–8, San Francisco, CA, USA, Jun. 2010.

[30] W. Kusakunniran, Q. Wu, J. Zhang, and H. Li. Speed-invariant gait recognition based on procrustes shape analysis using higher-order shape configuration. In *The 18th IEEE Int. Conf. Image Processing*, pages 545–548, 2011.

[31] W. Kusakunniran, Q. Wu, J. Zhang, and H. Li. Gait recognition under various viewing angles based on correlated motion regression. *IEEE Trans. Circuits Syst. Video Techn.*, 22(6):966–980, 2012.

[32] T. Lam and R. Lee. A new representation for human gait recognition: Motion silhouettes image (msi). In *Proc. of the IAPR Int. Conf. on Biometrics 2006*, pages 612–618, Jan. 2006.

[33] T. H. W. Lam, K. H. Cheung, and J. N. K. Liu. Gait flow image: A silhouette-based gait representation for human identification. *Pattern Recognition*, 44:973–987, April 2011.

[34] T. Lee, S. Ranganath, and S. Sanei. Fusion of chaotic measure into a new hybrid face-gait system for human recognition. In *Proc. of the 18th Int. Conf. on Pattern Recognition*, volume 4, pages 541–544,

Hong Kong, China, Aug. 2006.

[35] X. Li, S. Maybank, S. Yan, D. Tao, and D. Xu. Gait components and their application to gender recognition. *Trans. on Systems, Man, and Cybernetics, Part C*, 38(2):145–155, Mar. 2008.

[36] Y. Liu, R. Collins, and Y. Tsin. Gait sequence analysis using frieze patterns. In *Proc. of the 7th European Conf. on Computer Vision*, volume 2, pages 657–671, 2002.

[37] Z. Liu and S. Sarkar. Simplest representation yet for gait recognition: Averaged silhouette. In *Proc. of the 17th Int. Conf. on Pattern Recognition*, volume 1, pages 211–214, Aug. 2004.

[38] Z. Liu and S. Sarkar. Improved gait recognition by gait dynamics normalization. *IEEE Trans. on Pattern Analysis and Machine Intelligence*, 28(6):863–876, 2006.

[39] Y. Makihara, M. Hossain, D. Muramatsu, and Y. Yagi. Score-level fusion based on the direct estimation of the bayes error gradient distribution. In *Proc. of the Int. Joint Conf. on Biometrics (IJCB2011)*, pages 1–8, Washington D.C., USA, Oct. 2011.

[40] Y. Makihara, H. Mannami, A. Tsuji, M. Hossain, K. Sugiura, A. Mori, and Y. Yagi. The ou-isir gait database comprising the treadmill dataset. *IPSJ Trans. on Computer Vision and Applications*, 4:53–62, Apr. 2012.

[41] Y. Makihara, R. Sagawa, Y. Mukaigawa, T. Echigo, and Y. Yagi. Gait recognition using a view transformation model in the frequency domain. In *Proc. of the 9th European Conf. on Computer Vision*, pages 151–163, Graz, Austria, May 2006.

[42] Y. Makihara, R. Sagawa, Y. Mukaigawa, T. Echigo, and Y. Yagi. Which reference view is effective for gait identification using a view transformation model? In *Proc. of the IEEE Computer Society Workshop on Biometrics 2006*, New York, USA, Jun. 2006.

[43] Y. Makihara, A. Tsuji, and Y. Yagi. Silhouette transformation based on walking speed for gait identification. In *Proc. of the 23rd IEEE Conf. on Computer Vision and Pattern Recognition*, San Francisco, CA, USA, Jun 2010.

[44] Y. Makihara and Y. Yagi. Silhouette extraction based on iterative spatio-temporal local color transformation and graph-cut segmentation. In *Proc. of the 19th Int. Conf. on Pattern Recognition*, Tampa, Florida USA, Dec. 2008.

[45] D. Matovski, M. Nixon, S. Mahmoodi, and J. Carter. The effect of time on gait recognition performance. *Information Forensics and Security, IEEE Trans. on*, 7(2):543 –552, april 2012.

[46] A. Mori, Y. Makihara, and Y. Yagi. Gait recognition using period-based phase synchronization for low frame-rate videos. In *Proc. of the 20th Int. Conf. on Pattern Recognition*, pages 2194–2197, Istanbul, Turkey, Aug. 2010.

[47] S. Mowbray and M. Nixon. Automatic gait recognition via fourier descriptors of deformable objects. In *Proc. of IEEE Conf. on Advanced Video and Signal Based Surveillance*, pages 566–573, 2003.

[48] H. Murase and R. Sakai. Moving object recognition in eigenspace representation: Gait analysis and lip reading. *Pattern Recognition Letters*, 17:155–162, 1996.

[49] K. Nandakumar, Y. Chen, S. C. Dass, and A. K. Jain. Likelihood ratio-based biometric score fusion. *IEEE Trans. on Pattern Analysis and Machine Intelligence*, 30(2):342–347, 2008.

[50] J. Neyman and E. Pearson. On the problem of the most efficient tests of statistical hypotheses. *Philosophical Trans. of the Royal Society of London*, 231:289–337, 1933.

[51] M. S. Nixon, T. N. Tan, and R. Chellappa. *Human Identification Based on Gait*. Int. Series on Biometrics. Springer-Verlag, Dec. 2005.

[52] S. Niyogi and E. Adelson. Analyzing and recognizing walking figures in xyt. In *Proc. of IEEE Conf. on Computer Vision and Pattern Recognition*, pages 469–474, 1994.

[53] P. Phillips, D. Blackburn, M. Bone, P. Grother, R. Micheals, and E. Tabassi. Face recogntion vendor test. http://www.frvt.org,, 2002.

[54] N. Poh and S. Bengio. F-ratio client-dependent normalisation on biometric authentication tasks. In *IEEE Int'l Conf. Acoustics, Speech, and Signal Processing (ICASSP)*, pages 721–724, Philadelphia, 2005.

[55] N. Poh, G. Heusch, and J. Kittler. On combination of face authentication experts by a mixture of quality dependent fusion classifiers. In *Proc. of th 7th Int. Workshop on Multiple Classifier Systems*, pages 344–356, Prague, Czech Republic, 2007.

[56] N. Poh and J. Kittler. On the use of log-likelihood ratio based model-specific score normalisation in biometric authentication. In *In LNCS 4542, IEEE/IAPR Proc. Int'l Conf. Biometrics (ICB'07)*, pages 614–624, Seoul, 2007.

[57] N. Poh, J. Kittler, and T. Bourlai. Improving biometric device interoperability by likelihood ratio-based quality dependent score normalization. In *Prof. of the IEEE 3rd Int. Conf. on Biometrics: Theory, Applications and Systems*, pages 1–5, 2007.

[58] S. Sarkar, J. Phillips, Z. Liu, I. Vega, P. G. ther, and K. Bowyer. The humanid gait challenge problem: Data sets, performance, and analysis. *Trans. of Pattern Analysis and Machine Intelligence*, 27(2):162–177, 2005.

[59] G. Sathish, D. S.V.Saravanan, D. S. Narmadha, and D. S. U. Maheswari. Multi-algorithmic iris recognition. *Int. Journal of Computer Applications*, 38(11):13–21, January 2012. Published by Foundation of Computer Science, New York, USA.

[60] G. Shakhnarovich and T. Darrell. On probabilistic combination of face and gait cues for identification. In *Proc. Automatic Face and Gesture Recognition 2002*, volume 5, pages 169–174, 2002.

[61] G. Shakhnarovich, L. Lee, and T. Darrell. Integrated face and gait recognition from multiple views. In *Proc. of IEEE Conf. on Computer Vision and Pattern Recognition*, volume 1, pages 439–446, 2001.

[62] J. Shin and D. Han. Multi-classifier for wlan fingerprint-based positioning system. In *Proc. of The World Congress on Engineering 2010*, pages 768–773, 2010.

[63] J. Shutler, M. Grant, M. Nixon, and J. Carter. On a large sequence-based human gait database. In *Proc. of the 4th Int. Conf. on Recent Advances in Soft Computing*, pages 66–71, Nottingham, UK, Dec. 2002.

[64] R. Snelick, U. Uludag, A. Mink, M. Indovina, and A. K. Jain. Large scale evaluation of multimodal biometric authentication using state-of-the-art systems. *IEEE Trans. on Pattern Analysis and Machine Intelligence*, 27(3):450–455, March 2005.

[65] K. Sugiura, Y. Makihara, and Y. Yagi. Gait identification based on multi-view observations using omnidirectional camera. In *Proc. 8th Asian Conf. on Computer Vision*, pages 452–461, Tokyo, Japan, Nov. 18-22 2007. LNCS 4843.

[66] D. Tao, X. Li, X. Wu, and S. Maybank. Human carrying status in visual surveillance. In *Proc. of IEEE Conf. on Computer Vision and Pattern Recognition*, volume 2, pages 1670–1677, New York, USA, Jun. 2006.

[67] How biometrics could change security. http://news.bbc.co.uk/2/hi/programmes/click_online/ 7702065.stm.

[68] B. Ulery, W. Fellner, P. Hallinan, A. Hicklin, and C. Watson. Studies of biometric fusion. appendix c. evaluation of selected biometric fusion techniques. *NIST Interagency Report*, 7346:1–14, 2006.

[69] R. Urtasun and P. Fua. 3d tracking for gait characterization and recognition. In *Proc. of the 6th IEEE Int. Conf. on Automatic Face and Gesture Recognition*, pages 17–22, 2004.

[70] P. Wand and C. Jones. *Kernel Smoothing*. Monographs on Statistics and Applied Probability. Taylor & Francis, 1994.

[71] C. Wang, J. Zhang, J. Pu, X. Yuan, and L. Wang. Chrono-gait image: A novel temporal template for gait recognition. In *Proc. of the 11th European Conf. on Computer Vision*, pages 257–270, Heraklion, Crete, Greece, 2010.

[72] F. Wang and J. Han. Multimodal biometric authentication based on score level fusion using support vector machine. *Opto-Electronics Review*, 17(1):59–64, 2009.

[73] F. Wang, J. Han, and X. Yao. Iris recognition based on multialgorithmic fusion. *WSEAS Trans. Info. Sci. and App.*, 4(12):1415–1421, Dec. 2007.

[74] L. Wang, T. Tan, W. Hu, and H. Ning. Automatic gait recognition based on statistical shape analysis. *IEEE Trans. on Image Processing*, 12(9):1120–1131, 2003.

[75] Y. Wang, S. Yu, Y. Wang, and T. Tan. Gait recognition based on fusion of multi-view gait sequences. In *Proc. of the IAPR Int. Conf. on Biometrics 2006*, pages 605–611, Jan. 2006.

[76] C. Yam, M. Nixon, and J. Carter. Automated person recognition by walking and running via model-based approaches. *Pattern Recognition*, 37(5):1057–1072, 2004.

[77] H.-D. Yang and S.-W. Lee. Reconstruction of 3d human body pose for gait recognition. In *Proc. of the IAPR Int. Conf. on Biometrics 2006*, pages 619–625, Jan. 2006.

[78] S. Yu, D. Tan, and T. Tan. A framework for evaluating the effect of view angle, clothing and carrying condition on gait recognition. In *Proc. of the 18th Int. Conf. on Pattern Recognition*, volume 4, pages 441–444, Hong Kong, China, Aug. 2006.

[79] D. Zhang, Y. Wang, and B. Bhanu. Ethnicity classification based on gait using multi-view fusion. In *IEEE Computer Society and IEEE Biometrics Council Workshop on Biometrics 2010*, pages 1–6, San Francisco, CA, USA, Jun. 2010.

[80] T. Zhang, X. Li, D. Tao, and J. Yang. Multimodal biometrics using geometry preserving projections. *Pattern Recognition*, 41(3):805–813, 2008.

[81] X. Zhou and B. Bhanu. Feature fusion of side face and gait for video-based human identification. *Pattern Recognition*, 41(3):778–795, 2008.